Biophysical Journal
Article

Biophysical Society

Two-Tone Suppression of Simultaneous Electrical and Mechanical Responses in the Cochlea

Wei Dong[1] and Elizabeth S. Olson[2,*]
[1]VA Loma Linda Health Care System and Otolaryngology/Head & Neck Surgery, Loma Linda University, Loma Linda, California; and
[2]Otalaryngology/Head & Neck Surgery and Biomedical Engineering, Columbia University, New York, New York

ABSTRACT Cochlear frequency tuning is based on a mildly tuned traveling-wave response that is enhanced in amplitude and sharpness by outer hair cell (OHC)-based forces. The nonlinear and active character of this enhancement is the fundamental manifestation of cochlear amplification. Recently, mechanical (pressure) and electrical (extracellular OHC-generated voltage) responses were simultaneously measured close to the sensory tissue's basilar membrane. Both pressure and voltage were tuned and showed traveling-wave phase accumulation, evidence that they were locally generated responses. Approximately at the frequency where nonlinearity commenced, the phase of extracellular voltage shifted up, to lead pressure by >1/4 cycle. Based on established and fundamental relationships among voltage, force, pressure, displacement, and power, the observed phase shift was identified as the activation of cochlear amplification. In this study, the operation of the cochlear amplifier was further explored, via changes in pressure and voltage responses upon delivery of a second, suppressor tone. Two different suppression paradigms were used, one with a low-frequency suppressor and a swept-frequency probe, the other with two swept-frequency tones, either of which can be considered as probe or suppressor. In the presence of a high-level low-frequency suppressor, extracellular voltage responses at probe-tone frequencies were greatly reduced, and the pressure responses were reduced nearly to their linear, passive level. On the other hand, the amplifier-activating phase shift between pressure and voltage responses was still present in probe-tone responses. These findings are consistent with low-frequency suppression being caused by the saturation of OHC electrical responses and not by a change in the power-enabling phasing of the underlying mechanics. In the two-tone swept-frequency suppression paradigm, mild suppression was apparent in the pressure responses, while deep notches could develop in the voltage responses. A simple analysis, based on a two-wave differencing scheme, was used to explore the observations.

INTRODUCTION

The study of two-tone suppression in the cochlea has a long history, beginning with its observation in the cochlear microphonic (1), followed by observations in the auditory nerve (2). Two-tone suppression has been observed in basilar membrane (BM) motion (3–7) and those observations showed that most of the properties of neural two-tone suppression originate in the cochlea's nonlinear mechanics. It is generally believed that two-tone suppression arises when partial saturation of outer hair cell (OHC) mechano-transduction current at the suppressor frequency reduces the magnitude of OHC mechano-transduction current (and thus OHC voltage and OHC-based forces) at the probe frequency (6,8). The traveling-wave nature of cochlear mechanics is also needed to understand the observed suppression behavior: a high-frequency-side suppressor of a frequency that does not even reach a given location is nevertheless able to suppress the response to a lower frequency probe tone, providing the high frequency tone does reach locations at which the lower frequency tone scales nonlinearly with stimulus level (9). Thus, to first order, two-tone suppression is understood to be a predictable outcome of the saturation of OHC-enhanced traveling-wave cochlear mechanics (10). However, questions remain. There are unexplained differences between neural and BM suppression—for example, the neural responses can be suppressed much more than the overall motion responses (4,7,9). Fundamental questions also remain regarding how the cochlear nonlinearity that underlies suppression is controlled, and regarding the relationship between BM motion and OHC excitation. Our study explores these questions.

Pressure and voltage responses were measured simultaneously, at the same location close to the BM, as described in Dong and Olson (11) and Fig. 1. Single-tone responses

Submitted April 22, 2016, and accepted for publication August 15, 2016.
*Correspondence: eao2004@cumc.columbia.edu
Editor: James Keener.
http://dx.doi.org/10.1016/j.bpj.2016.08.048

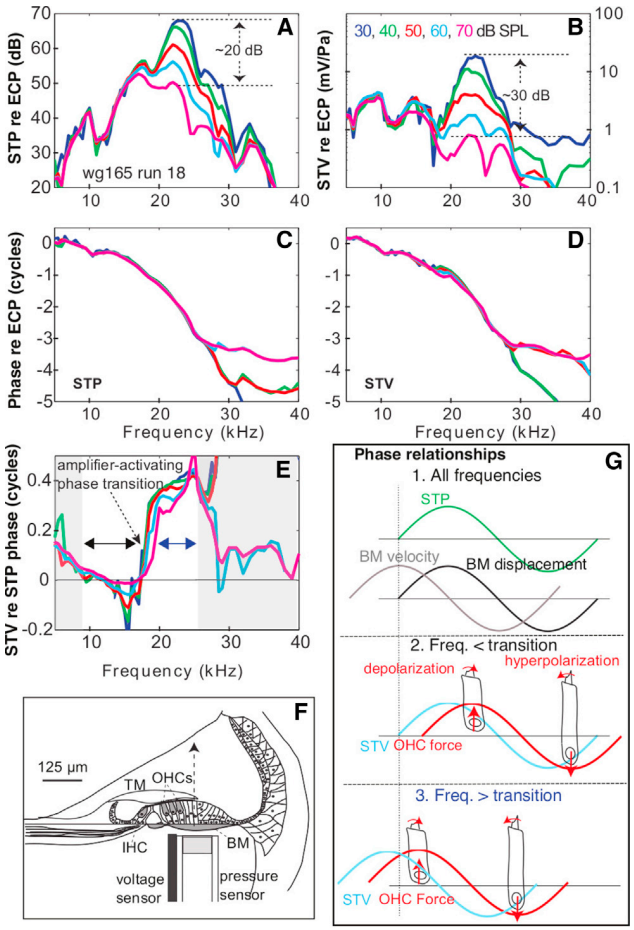

FIGURE 1 STP and STV measured close to the BM with single-tone stimulation. SPL color-coding is in (*B*). Single-tone responses show the tuned, nonlinear character of the (*A*) STP and (*B*) STV at the BM, here plotted normalized to ECP. (*C* and *D*) Phases referenced to ECP. Traveling-wave phase accumulation was present in both STP and STV through ~25–30 kHz. (*E*) STV-STP phase difference was close to 0 cycles from 8 to ~17 kHz, then underwent a rapid transition to ~0.35 cycles. The shaded region to the right in (*E*) is above the frequency for which traveling-wave phase accumulation ended (*C* and *D*) and thus the fast pressure mode is dominant. The shaded region to the left in (*E*) is also significantly influenced by the fast mode. These regions are not informative for the main points of this figure. (*F*) Cartoon of dual probe close to the organ of Corti. (*G*) Phase relationships that identify phase transition in (*E*) with cochlear amplification. The vertical line indicates phase zero of STP. "ECP" indicates ear canal pressure. To see this figure in color, go online.

are reviewed in the Results and Fig. 1; here we give a skeletal introduction. Scala tympani pressure (STP) close to the BM displays a tuned, nonlinear traveling wave response (Fig. 1, *A* and *C*) and is closely aligned with BM displacement. Voltage in the scala tympani (ST) at the BM (STV) is a measure of OHC mechano-transduction current, flowing through the primarily resistive electrical impedance of the cochlear bulk tissue (Fig. 1, *B* and *D*). The STV exhibited traveling-wave phase accumulation, identifying it as a response from local OHCs. In past work STP and STV were used to explore the relationship between the cochlea's mechanical nonlinearity and the OHC-based forces that produce it. In this study, the operation of the cochlear amplifier was further explored in the responses of the STP and STV to two-tone stimulation. Two different two-tone suppression paradigms were used, one with a low-frequency suppressor and a swept-frequency probe, the other with two swept-frequency tones of equal level, and fixed frequency ratio. The results of the low-side suppression study reinforced the OHC-current-saturation explanation for suppression, and added to our understanding of amplifier activation. The two-swept-frequency-tone suppression study was relatively exploratory, and its results unanticipated. Mild suppression was apparent in the pressure responses, while deep notches could develop in the STV responses at frequency f_1 (lower frequency) when f_2 (higher frequency) was close to the best frequency (BF) of the measurement location. These response notches are likely caused by motions within the cochlear partition that excite OHCs. Measurements using optical coherence tomography (OCT) have observed differential motion between intracochlear structures (e.g., (12–14)), and cochlear models show that these different motions could be due to coupled traveling waves on the tectorial membrane (TM) and BM (15–17). The OCT results, as well as two-scala pressure measurements in scala media and ST, indicate fairly tightly coupling between TM and BM traveling waves (18). Motivated by these experimental findings and modeling predictions, we constructed a simple schematic of coupled-traveling-wave-based OHC stimulation, derived from physics-based cochlear models, that was useful for understanding our observations.

MATERIALS AND METHODS

The experiments were approved by Columbia University's Institutional Animal Care and Use Committee. The experiments were performed in young adult gerbils anesthetized with pentobarbital and euthanized at the end of the experiment. The cochlea was exposed by opening the bulla via a ventral approach and the dual pressure-voltage sensor was inserted into a hand-drilled hole, ~200 μm in diameter, made in the ST of the basal turn of the cochlea where the BF is ~20 kHz (11). The dual sensor is based on fiber-optic pressure sensors (19,20). It is composed of a pressure sensor, 125 μm in diameter, with an isonel-coated platinum wire, 28 μm in diameter, adhered to its side, with the tip of the electrode flush with the pressure sensing tip (Fig. 1 *F*). Both the pressure sensor and the wire electrode had frequency responses that were approximately flat over the frequency range of measurement (11). A silver reference electrode for the voltage sensor was connected to the neck muscle. The sensor was advanced in micrometer steps until contacting the BM (determined by the sudden appearance of a noisy signal on the oscilloscope), then retracted ~10 μm. The data reported here were taken at that location, close to the BM. The sensor's perturbation has been examined previously, primarily via measurements of compound action potential thresholds (21,22). Based on the observations in those studies, perturbation is reasonably small.

Single tones and tone pairs were generated with the System III (Tucker-Davis Technologies, Alachua, FL), running purpose-built programs written with the Visual Design Studio (Tucker-Davis) and the software MATLAB (The MathWorks, Natick, MA). The tones, of 1–2 s duration, were delivered to the ear canal (EC) in a closed field configuration via one or two RadioShack speakers (Fort Worth, TX). A Sokolich ultrasonic microphone

was used to calibrate and measure the sound pressure level in the EC close to the tympanic membrane. Sound pressure level (SPL) is reported as dB SPL (decibels relative to 20 μPa peak). Two two-tone suppression paradigms were used. In the first, the suppressor frequency was much lower than the ~20 kHz BF at the location of measurement: a 4 kHz tone served as suppressor and a second tone, whose frequency was varied sequentially from 1 to 40 kHz in steps of ~0.5 kHz, served as probe. We emphasize data from 5 to 40 kHz, for which the 4 kHz tone is a low-side suppressor. In the second paradigm, two equal SPL tones were delivered at a fixed frequency ratio that varied in different data sets from 1.05 to 1.35. These ratios were chosen to be similar to our previous studies (21). The frequencies of the tone pairs were increased sequentially from ~1 to 40 kHz in ~0.5 kHz steps and are referred to as "swept-frequency" tones. Responses were time-averaged and analyzed via Fourier transform offline using MATLAB.

RESULTS

As an introductory note, at high SPL and in frequency regions significantly above the BF, the STV response cannot be considered as solely generated by local OHCs, because of current spread from other locations. The space constant is ~80 μm (11,23). In addition, at frequencies above the BF, the STP response becomes dominated by the fast, compression pressure mode, which is not involved in cochlear excitation, at least to first order (24–26). Frequency regions of interest—those in which STV responses are local and STP responses are dominated by the slow, traveling wave—are those in which the phase-versus-frequency of these responses shows traveling-wave accumulation. We restrict our analysis to those regions. At high SPL and in less active (slightly damaged) preparations, STP becomes fast-mode-dominated at relatively low frequencies (22). Suppression has an effect similar to high SPL, and this restricted the number of preparations for presentation—those that possessed a frequency range of slow-mode domination that was wide enough for the analysis. Two-tone suppression experiments were performed in fourteen cochleae. Seven were passive preparations due to loss of sensitivity when opening the cochlea. Results from three preparations are shown and the results from the active preparations were consistent with the findings presented here.

An example of single-tone responses

Our recent single-tone measurements provide background for the two-tone results (11) and we briefly review the most important findings here. An example from the ~24 kHz BF place is in Fig. 1. The STP and STV amplitude responses, normalized to EC pressure, display the familiar, tuned nonlinearity (Fig. 1, *A* and *B*) and traveling wave phase accumulation through several cycles (Fig. 1, *C* and *D*). These observations indicate that STP and STV were tied to the stimulus and response of hair cells that were local to the sensing tip (Fig. 1 *F*). STP is a mechanical drive to organ of Corti motion and thus hair cell stimulation, and in a broad frequency range that includes the BF peak, is approximately proportional to BM displacement (11,27). (At frequencies <~8 kHz, this simple proportionality is less applicable due to the influence of the fast pressure mode (18).) The extracellular STV is a measure of OHC mechano-transduction current, flowing through the primarily resistive electrical impedance of the cochlear bulk tissue. OHC force is related to OHC current as described below.

The relative response phases are informative. We have shown that positive STP is approximately in phase with BM displacement toward scala vestibuli (11,27) and velocity always leads displacement by 90°. These relationships are illustrated in the green, black, and gray curves of Fig. 1 *G*. Due to OHC membrane capacitance, OHC voltage lags OHC current, and thus lags STV. Based on Johnson et al. (28), that phase lag is ~60° at BF and smaller at lower frequencies. Others have shown that OHC electromotile force is approximately in phase with OHC voltage: depolarizing (positive) OHC voltage produced a contractile force (which would be up on the BM) (29). Finally, in our measurements, the STV phase relative to STP phase underwent a transition to a >90° lead at ~17 kHz (Fig. 1 *E*). The phase relationships below and above the transition are illustrated in the red and blue curves of Fig. 1 *G*. Considering all those relationships, at frequencies below the transition (*middle section* of Fig. 1 *G*), OHC upward force lags upward BM velocity by >90°. However, at frequencies above the transition (*lower section* of Fig. 1 *G*), OHC upward force leads BM upward displacement and is substantially in phase with upward BM velocity. From fundamental principles, when force is in phase with velocity, power is transferred: OHC forces will transfer power to the BM and amplify traveling wave motion. Thus, the phase transition of Fig. 1 *E* activates the cochlear amplifier (11). Consistent with the concept of amplifier activation, nonlinearity in Fig. 1, *A* and *B*, commenced approximately at the frequency of the phase transition and was present throughout the frequency range for which STV led STP.

The amplifier-activating phase transition was present throughout the SPL range, even at high SPL where the degree of nonlinearity was relatively small. We concluded that the phase shift was based in passive mechanics, and set the conditions necessary for amplification, while the size of the amplification, which diminishes in relative terms as SPL increases, was limited by the saturation of OHC mechano-transduction current. A greater degree of nonlinearity was observed in STV than STP (compare the panels of Fig. 1, *A* and *B*), which is as expected when saturation of OHC current is the basis for the nonlinearity.

Based on these observations from single-tone responses, we hypothesized that the presence of the high-SPL, low-frequency suppressor would reduce cochlear nonlinearity, but the amplifier-activating phase shift would remain.

High-SPL, low-frequency suppressor

The effects of a low-frequency suppressor are shown from two preparations. Fig. 2 illustrates how a high-SPL,

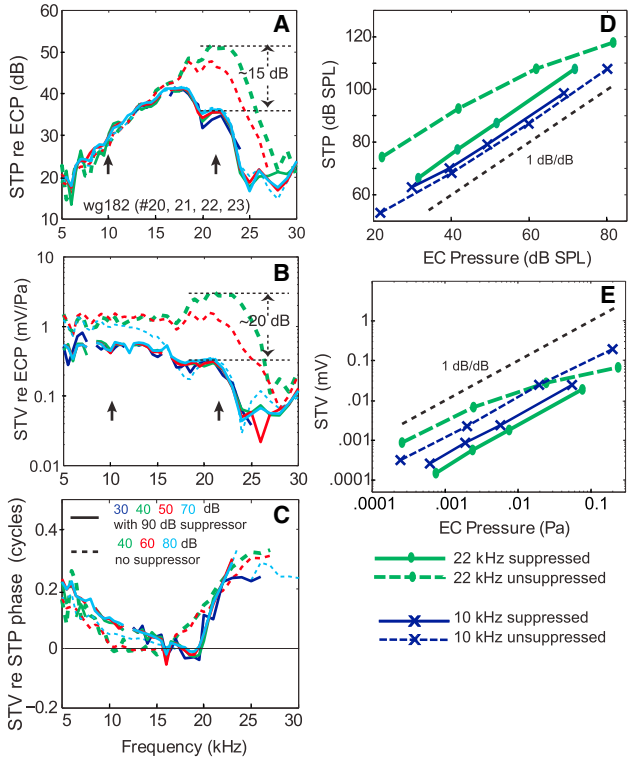

FIGURE 2 Effects of a 90 dB SPL low-frequency (4 kHz) suppressor on swept-frequency probe tones of various levels. (*A–C*) Key is in (*C*). (*A*) Normalized amplitude of STP measured at a location close to the BM. (*B*) Normalized amplitude of STV measured at the same time and location. (4 kHz harmonics were large in some responses and were distracting and thus are excluded, resulting in the gaps in the plotted data.) Bold arrows in (*A*) and (*B*) identify the frequencies of the responses plotted as input-output functions in (*D*) and (*E*). (*C*) STV-STP phase difference. Input-output functions at 10 and 22 kHz, with EC pressure the input, and output (*D*) STP and (*E*) STV. To see this figure in color, go online.

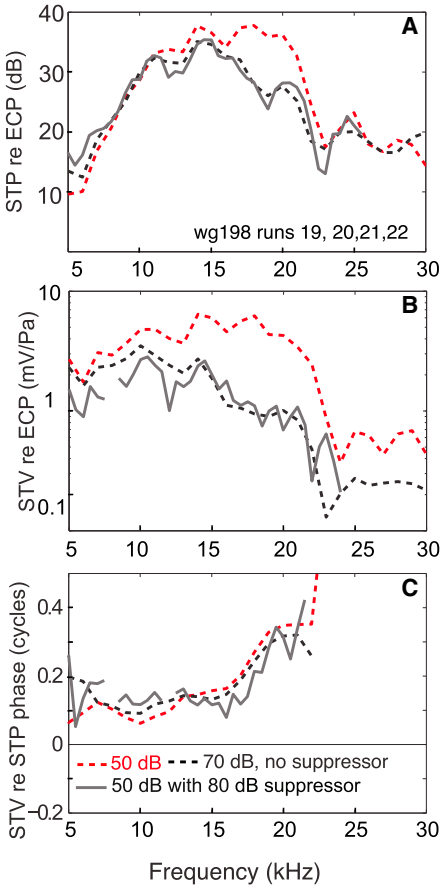

FIGURE 3 Effects of an 80 dB SPL low-frequency (4 kHz) suppressor on 50 dB SPL swept-frequency probe tones. Key is in (*C*). (*A*) Normalized amplitude of STP measured at a location close to the BM. (*B*) Normalized amplitude of STV measured at the same time, and same location. (4 kHz harmonics were large in the voltage responses and were distracting and thus are excluded, resulting in the gaps in the plotted data.) (*C*) STV-STP phase difference. To see this figure in color, go online.

low-frequency tone (90 dB SPL at 4 kHz) suppressed probe-tone responses to swept-frequency stimuli delivered over a range of SPL. In the experiment of Fig. 3 a low-frequency (4 kHz) suppressor tone was delivered over a range of SPLs (50–80 dB SPL), and probe-tone responses to swept-frequency stimuli, delivered at the single level of 50 dB SPL, were measured. As a comparison, single-tone responses (no suppressor condition), are plotted in dashed lines in both figures. The responses are shown normalized to the pressure in the EC.

In the absence of a suppressor, the single-tone STP responses show the familiar saturating nonlinearity, starting at ~16 kHz (*dashed colored lines* in Fig. 2 *A*). The BF was ~22 kHz and at that frequency from 40 to 80 dB SPL there was ~15 dB of nonlinear compression. STV possessed a greater degree of compression than STP (*double-headed arrows* in Fig. 2, *A* and *B*), and at the highest SPL, 80 dB SPL, the range of nonlinear compression in STV extended down in frequency to ~12 kHz. When suppressed with the 90 dB SPL, 4 kHz tone, both the STP and the STV swept-frequency responses were linearized: at all levels of the probe tone, the normalized responses lay on top of each other (*solid lines* in Fig. 2, *A* and *B*). The suppressed STP responses also lay on top of the high-level (80 dB SPL) single-tone responses (Fig. 2 *A*). In contrast, the suppressed STV responses lay at a level below the high-level (80 dB SPL) single-tone responses (Fig. 2 *B*), at frequencies up to ~17 kHz.

The input-output functions in Fig. 2, *D* and *E*, highlight differences in the nonlinear peak region and the low-frequency linear region, using 22 kHz and 10 kHz for illustration (*bold arrows* in Fig. 2, *A* and *B*). At 22 kHz in both STV and STP, the unsuppressed responses were nonlinear (*green dashed*) and the suppressed responses were reduced (shifted vertically) and linearized: the suppressed curves have slopes of 1 dB/dB (*green solid*). At 10 kHz, both unsuppressed and suppressed responses were linear—they have slopes of 1 dB/dB (*blue curves*). In STP, the 10 kHz unsuppressed and suppressed curves almost overlay; a very small upward

vertical shift is seen in the suppressed curve (Fig. 2 *D*). In contrast, in STV the 10 kHz suppressed curve was shifted downward substantially from the unsuppressed curve (Fig. 2 *E*). This aspect of STV's behavior is as predicted for a saturating nonlinearity, and will be discussed below.

In the single-tone responses the STV-STP phase difference underwent the familiar transition from ~0 to ~0.3 cycles at frequencies where mechanical nonlinearity began, ~17 kHz (*dashed lines* in Fig. 2 *C*). This is the phase transition that activates the amplifier as in Fig. 1 *E*. The phase transition was similar for the single-tone responses at 40 and 60 dB SPL (*green* and *red dashed lines* in Fig. 2 *C*) and at 80 dB SPL it became more abrupt and shifted to slightly higher frequencies but its fundamental character, transitioning from ~0 to 0.3 cycles, persisted (*blue dashed line* in Fig. 2 *C*). In the suppressed case, the STV-STP phase had the same character as the high-SPL unsuppressed case (*solid lines* in Fig. 2 *C*). Thus, as we hypothesized, the amplifier-activating phase transition was retained with the low-frequency suppressor, even though the mechanical responses to the probe tone were no longer amplified.

This result was confirmed in another preparation (Fig. 3), in which a 50 dB SPL swept-frequency probe tone was presented along with a 4 kHz suppressor at levels from 50 to 80 dB SPL. The suppressor at levels of 50, 60, and 70 dB SPL did not affect the probe-tone responses in either STP or STV so those responses are not shown (STP or STV responses lay on top of the *red dashed curves* showing the unsuppressed responses). In the presence of the 80 dB SPL suppressor, the 50 dB SPL probe-tone responses, both STP and STV, were suppressed (*gray solid line*): they look much like the single-tone responses to 70 dB SPL (*black dashed lines*). However, as in the case of Fig. 2, in the low-frequency region of linear mechanics, suppressed STV responses were reduced compared to the single-tone STV responses (Fig. 3 *B*, compare *gray solid* to *black dashed lines* at frequencies <10 kHz). Finally, consistent with our hypothesis, the amplifier-activating STV-STP phase transition was present in the probe tone in both the suppressed and unsuppressed responses (Fig. 3 *C*).

Two swept-frequency tones

In the second suppression paradigm, with two swept-frequency tones of fixed frequency ratio, mild suppression was apparent in the STP responses, with f_1 suppressed more than f_2. The most interesting observation was that deep notches could develop in the f_1 component of the STV responses at moderate stimulus levels. Examples are shown from two preparations in Figs. 4, 5, and 6.

Fig. 4 shows data at three stimulus levels (L1 = L2 = 50, 60, 70 dB SPL) and f_2/f_1 ratio of 1.25. At stimulus levels below 50 dB SPL suppression was not observed with this stimulus paradigm. The f_2 responses showed only a small degree of suppression compared to single-tone responses—thus the f_2 responses (*dashed lines*) can be approximately considered to be an unsuppressed comparison for the f_1 responses (*solid lines*). The f_1 STP was suppressed by up to ~6 dB in the region of nonlinear responses at ~24 kHz BF (Fig. 4 *A*) and in the STV a deep notch could develop in f_1 due to the

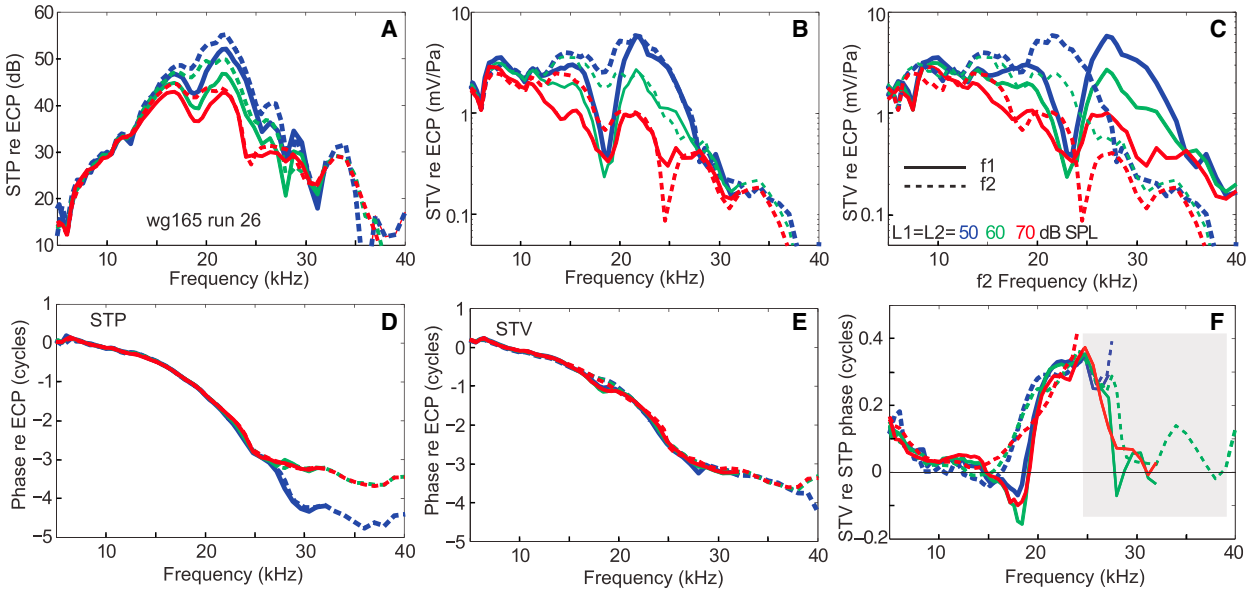

FIGURE 4 Two-swept-frequency-tone responses at three different stimulus levels. Key is in (*C*). (*A* and *D*) STP normalized amplitude and phase for ECP. (*B* and *E*) STV normalized amplitude and phase for ECP. For (*A*) and (*B*) and (*D–F*), the responses are plotted versus their own frequency on the *x* axis. (*C*) STV data as in (*B*), but here the f_1 responses are plotted versus the f_2 frequency on the *x* axis. (*F*) STV-STP phase difference. The f_2/f_1 ratio was 1.25 and f_2 and f_1 levels were 50, 60, and 70 dB SPL as indicated in the line colors. In the shaded area, the pressure responses were beginning to be dominated by the fast wave and are thus complicated to interpret and can be neglected. To see this figure in color, go online.

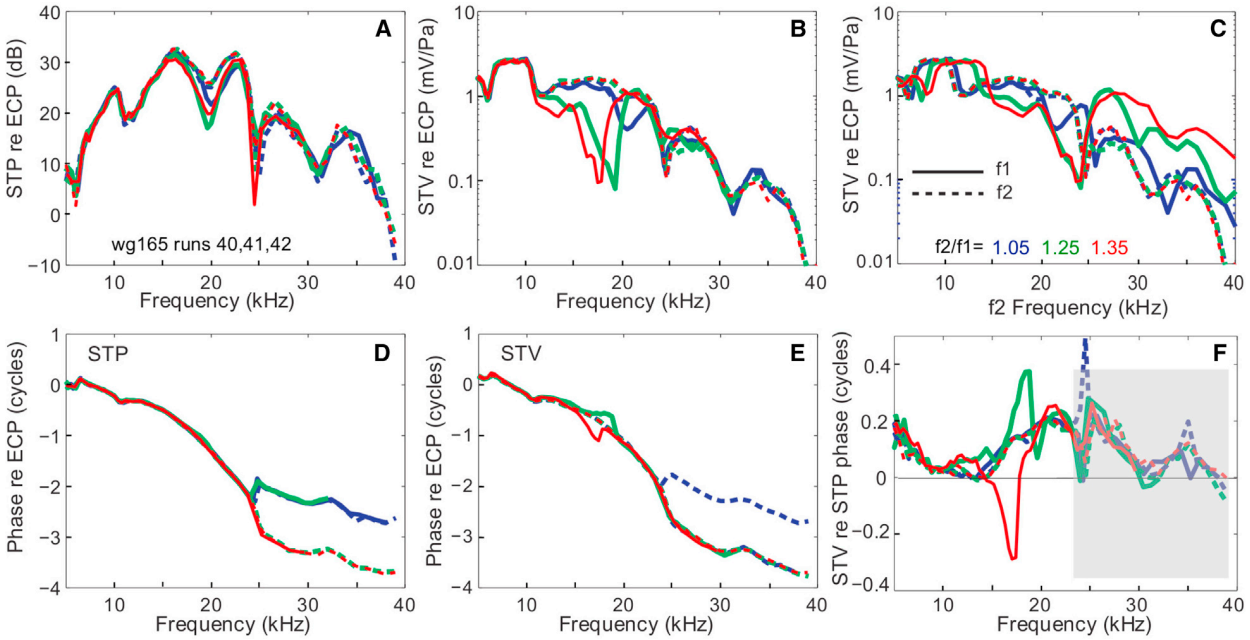

FIGURE 5 Two-tone swept-frequency responses with f_2/f_1 ratios 1.05, 1.25, and 1.35 and L1 = L2 = 60 dB SPL. (*A–F*) Panels arranged as in Fig. 4. Data were taken several hours after those of Fig. 4. Deep f_1 suppression notch is still apparent. To see this figure in color, go online.

presence of f_2 (Fig. 4 *B*). The deep notch in f_1 occurred when f_2 was close to the BF, an observation that is most evident in Fig. 4 *C*, where the f_1 response is plotted versus f_2 and the notch in f_1 is seen to approximately coincide with the BF in f_2. The phase difference of STV-STP varied at frequencies where the deep notch occurred (Fig. 4 *F*), but the phase transition to activate the cochlear amplifier remained. In many of the suppressed f_1 responses, when the phase shift began, it briefly shifted negative rather than positive, then reversed to retain a final positive excursion similar to that of the unsuppressed response (here represented by the f_2 response in *dashed lines*).

In a later data set from this preparation (Fig. 5) the cochlea had deteriorated somewhat, but the basic suppression observations noted in Fig. 4 remained. In Fig. 5, three f_2/f_1 ratios are shown, 1.05, 1.25, and 1.35, with L1 = L2 = 60 dB

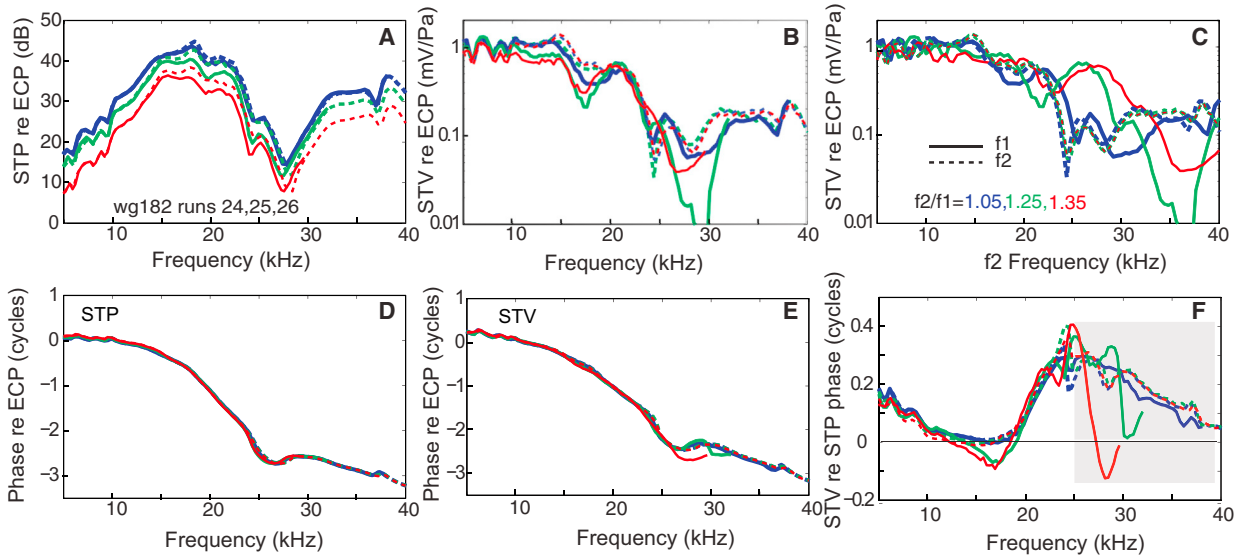

FIGURE 6 Two-tone swept-frequency responses with f_2/f_1 ratios 1.05, 1.25, and 1.35 and L1 = L2 = 70 dB SPL. (*A–F*) Panels arranged as in Fig. 4. (In *A*, STP normalized to EC pressure, the frequency-independent vertical shift indicates the pressure sensor was losing sensitivity, thus the quantitative results are uncertain in *A*.) To see this figure in color, go online.

SPL. (As noted above, the f_2 response was nearly unsuppressed and can be used as a reference. The f_2 response is plotted with *dashed lines*.) As in Fig. 4, there was mild suppression of the f_1 response in the STP, and a deep notch in the f_1 response in the STV at f_2/f_1 ratios of 1.25 and 1.35. Another observation from Figs. 4 *F* and 5 *F* is that the f_1 STV-STP phase could become oddly structured in the presence of f_2. The source of the structure is the STV phase (Figs. 4 *E* and 5 *E*).

In Fig. 6, a data set from another preparation confirmed the results from the preparation of Figs. 4 and 5. The observations are not as strong in this preparation, but the basic findings are confirmed: at ~17 kHz, the f_1 STV response developed a notch in the presence of f_2 and the STV-STP phase underwent a negative dip that preceded its positive transition.

DISCUSSION

Two-tone stimuli are a first step beyond single tones for exploring peripheral processing of the multifrequency sounds in the acoustic environment. Mechanical measurements of two-tone suppression have concentrated on BM motion, which was accessible to measurement. However, hair cells are stimulated at their apices, by the shearing motion of the stereocilia. BM motion, while closely related to the mechanical stimulus to stereocilia, is only one side of the stimulus equation. The relationship between STP at the BM (which is closely related to BM displacement) and STV at the BM (which is proportional to local OHC mechano-transduction current) informed our understanding of OHC stimulation, and how it is altered with two-tone stimulation.

High-SPL, low-frequency suppression

Basic observations

In the presence of a high-SPL low-frequency suppressor: 1) STP probe-tone responses were reduced in the nonlinear BF region and when fully suppressed, resembled passive responses; 2) STV probe-tone responses were reduced in the BF region as well as at frequencies far below the BF; and 3) the phase shift between STV and STP probe-tone responses did not change in its basic character; in particular, the amplifier-activating phase transition was still present. Findings 1) and 2) are consistent with previous work (e.g., Ruggero et al. (5) and Engebretson and Eldredge (30)). Combined with these, finding 3) reaffirms that low-frequency suppression is caused primarily by the saturation of OHC electrical responses by showing that it is not accompanied by a change in the amplifier-activating phasing of the underlying mechanics.

Shift in linearity

The concept that two-tone suppression is based on saturation of OHC mechano-transduction is bolstered by the observation (Figs. 2 and 3) that in the absence of suppression, the well-sub-BF STV response (the frequency region in which mechanics were linear) was linear through fairly high SPL, and when suppressed by a high-level low-frequency tone, the linear region in STV remained linear (normalized curves overlaying) but the transfer function (gain) values were reduced. This observation was illustrated in Figs. 2 *B* and 3 *B* at frequencies up to ~17 and 12 kHz respectively, and in Fig. 2 *E*'s 10 kHz curves. This observation was made in cochlear microphonic responses early in the study of two-tone suppression (31) and it was noted to be the expected result of a saturating nonlinearity (Engebretson and Eldredge (30); see also Fahey et al. (32)). To illustrate the theoretical prediction, Fig. 7 *B* shows the input-output curve of a probe tone processed through one of the nonlinearities proposed by Fahey et al. (32) (their Fig. 3 *B*, our Fig. 7 *A*) in the presence (*green*) or absence (*blue*) of a second large tone of fixed input level (suppressor shown in *red* in Fig. 7 *B*). The probe-tone response was

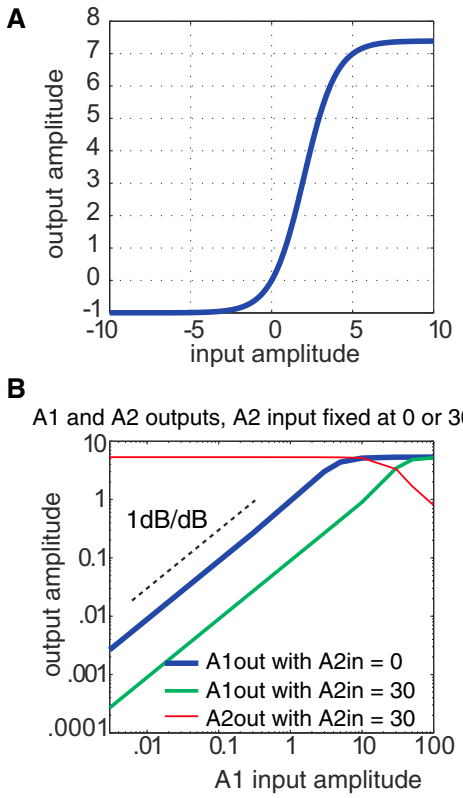

FIGURE 7 Input-output relationships from a saturating nonlinearity. (*A*) Nonlinear function. (*B*) Log-log plot of output for given input. A1 and A2 are signals of two different frequencies. For the simple static nonlinearity used to generate this figure, the frequency values and units are of no significance. $A2_{in}$ is the amplitude of the suppressor tone, which was at a value of either 30 (large) or zero. $A1_{in}$ was varied through the range noted on the *x* axis, and $A1_{out}$ is plotted in the absence (*blue*) and presence (*green*) of the A2 suppressor. On a log-log plot, the vertical position indicates the gain of the input-output relationship. To see this figure in color, go online.

linear through a wide range whether suppressed or unsuppressed—this is apparent in the slope of 1 dB/dB for both curves in the log-log plot (*dashed line* in Fig. 7 *B*). However, the input-output gain, represented by the *y* intercept in the log-log plot, is smaller for the suppressed tone (*green* in Fig. 7 *B*). This matches the observation from our well-sub-BF STV data, plotted as an input-output curve in Fig. 2 *E*. The well-sub-BF region is a region in which mechanical amplification is not activated (it is below the transition of Fig. 1 *E*) and so this change in gain is not expected to affect mechanical responses, consistent with the results. Thus, the vertical shift of the 10 kHz STV input-output curve (Fig. 2 *E*) does not require any consideration of cochlear amplification, it is simply a consequence of the saturation of the transducer current.

Two swept-frequency tones

Basic observations

In the two-swept-frequency-tone suppression paradigm, a prominent notch appeared in the f_1 STV response, close to the frequency where the STV-STP phase underwent the amplifier-activating phase transition. In fact, deep suppression notches in extracellular voltage and IHC potentials have been observed previously (33–35). Those authors observed that when a suppressor tone was presented within a narrow frequency range near BF, a probe tone would be suppressed, resulting in a notchlike suppression curve, which is similar to our observation. Their extracellular voltage measurements were not made very close to the BM, and they were cautious in their interpretation of those results. To explore the result in our local STV measurement, we start by noting that even in the single-tone measurements, the STV phase transition was often accompanied by a dip or notch in the STV amplitude. An example of a STV amplitude dip is in the 40- and 50 dB SPL results at ~17.5 kHz (Fig. 1 *B*). In the swept-frequency suppression experiments, this notch sometimes became pronounced in the f_1 responses, as in Figs. 4, 5, and 6, and at the same time the STV-STP phase transition could become oddly shaped, due to additional phase structure in STV. In the analysis of Dong and Olson (11), we showed with a cable model that STV notches and phase shifts above the BF could be attributed to cancellation of current between local and distant OHCs (see also Fridberger et al. (23)), but that the STV phase shift below the BF was in a region in which the traveling-wave wavelength was too long to produce phase cancellation from adjacent regions. Thus, we concluded that a different mechanism was responsible for phase shifts and amplitude notches at frequencies below BF. We noted that the STV-STP transition (Fig. 1 *E*) led to phasing that allowed for power input from the OHCs into the traveling wave in the frequency region above the transition, but did not propose a mechanism for the transition. The swept-frequency, two-tone results allow for informed speculation about the mechanism.

A simple schematic model

With the swept-frequency two-tone results adding information, we propose a simple mechanism for the amplifier-activating phase transition we have emphasized (Figs. 1 *E*, 2 *C*, 3 *C*, 4 *F*, 5 *F*, and 6 *F*). Several cochlear models have been developed in which the TM and BM are treated as separate structures that are coupled by the mechanics of the organ of Corti. In these models, when the TM and BM were loosely coupled their motions differed considerably and when they were tightly coupled they moved relatively similarly (15,17). The physics-based model of Cormack et al. (15) predicted TM and BM motions with similar but not identical amplitudes and phases. At frequencies well below the BF, the TM amplitude was approximately the same size as that of the BM and then grew to be larger close to the BF. These two-wave models were based on passive mechanics, and recent measurements of passive pressure close to the cochlear partition in scala media and ST indicate that the partition structures are closely coupled (18). In active preparations in which the motions of the BM and TM and/or reticular lamina have been measured using OCT, either simultaneously or in close sequence, coupling also appears to be quite tight. For example, reticular lamina re: BM phase leads of ~30° at frequencies around BF were observed in the guinea pig base (12), and similarly sized phase lags noted for TM re: BM motions in the mouse apex (13). A recent article by Lee et al. (14), confirmed phase differences of fairly small magnitude at frequencies up to the BF. For the purposes of this contribution, it is most important to note that based on the available data, motions within the partition are fairly tightly coupled.

The STV represents OHC mechano-transduction current, which is due to the differential motion at the top and bottom of the OHC hair bundle. In a simple two-wave model, this can be represented by the difference between the motions of the BM and TM. (A recent elaboration of a two-wave model described a more realistic TM shearing motion (16).) A notch in OHC mechano-transduction current will occur at a location-frequency-SPL combination for which the TM and BM motions are approximately the same size and same phase. Thus this schematic model can produce deep notches from the differencing of mildly structured responses, but is not capable of producing sharp peaks.

With this background, we take the difference between schematized BM and TM motions to find a BM-TM response. This is a complex difference, in which we first convert BM and TM response amplitude and phase into real and imaginary parts, take the difference $(BM_R - TM_R) + i(BM_i - TM_i)$ and convert back to amplitude and phase, for the resulting differential motion. We use this BM-TM quantity as a measure of OHC mechano-transduction current and thus extracellular voltage, STV. Fig. 8, *A–C*,

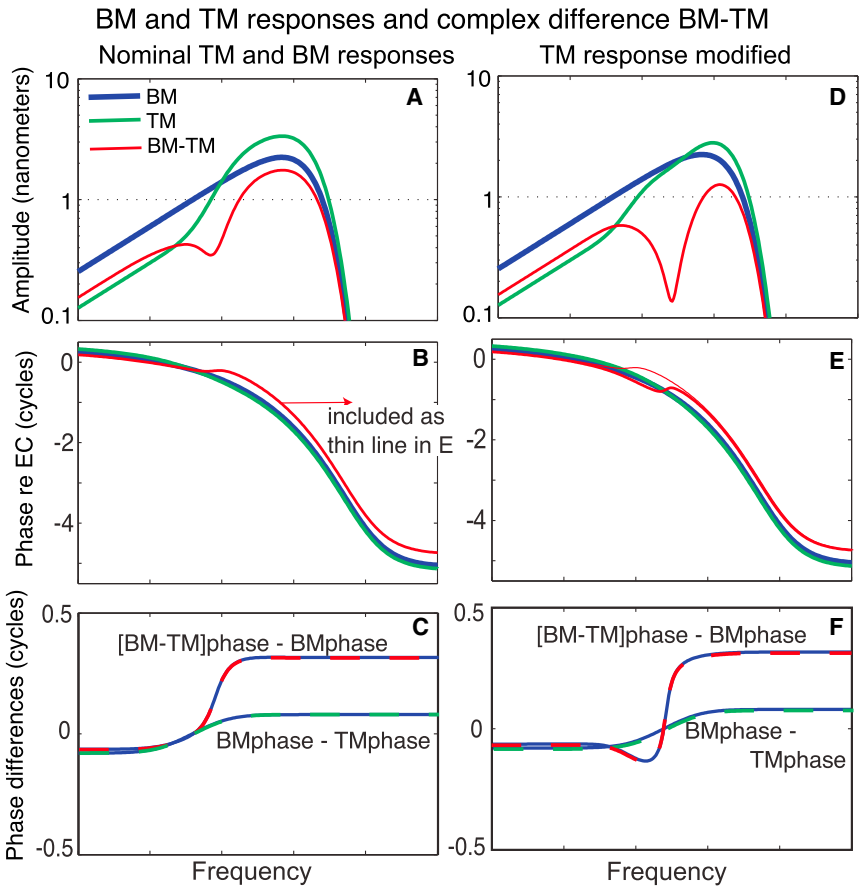

FIGURE 8 A simple schematic model to predict STV based on the difference between the motions of the BM and TM, [BM-TM]. BM responses represent our STP data, [BM-TM] represents OHC current, and thus the STV data. (*A–C*) Single-tone swept-frequency responses. (*D–F*) Swept-frequency responses in the presence of a suppressor, which was taken to modify TM motion slightly. (*A* and *D*) Motion amplitude of the BM, TM, and [BM-TM] without (*A*) and with (*D*) suppression; (*B* and *E*) phases of the BM, TM, and [BM-TM] motions without (*B*) and with (*E*) suppression; and (*C* and *F*) phase differences: [BM-TM] phase for BM phase and BM phase for TM phase without (*C*) and with (*F*) suppression. To see this figure in color, go online.

gives an example from this simple scheme, first used to model single-tone responses. The *x* axis is frequency, and the concept of scaling symmetry was used to convert from a space to a frequency axis (36). The blue BM curve is a reasonable representation of the frequency response of the BM motion. As noted above, STP at the BM, and BM displacement are quite similar in a broad frequency region including the BF peak, and the blue curve is loosely based on both BM responses from the literature and our own STP data. As derived from the physics-based model (15), the TM motion goes from being smaller to being greater than BM motion as the frequency increases, close to the BF (*green* in Fig. 8 *A*). In the BM-TM curve representing STV (*red* in Fig. 8 *A*), there is a gentle notch, and in the BM-TM re: BM phase there is a slightly less than half-cycle phase transition (*red* and *blue curves* in Fig. 8 *C*)—behavior that is similar to the single-tone STV amplitude and STV re: STP phase results in Fig. 1, *B* and *E*.

The difference of two similar quantities is very sensitive to those two quantities, and with small changes in either of the original quantities, the BM-TM motion difference (representing STV) can display deep notches and unusual phase shifts. This is what is needed to produce the observations of our two-swept-frequency-tone suppression STV data. To produce suppressed STV results in the schematic we introduced a small change in TM motion, which might be caused by a change in the coupling between the BM and TM, for example. An illustration is in Fig. 8, *D–F*. Consider these as the f_1 responses, and imagine that the presence of the f_2 suppressor had the observed effect on the TM motion (compare to the unmodified (unsuppressed) responses in Fig. 8, *A–C*). With a small change in TM motion, a deep notch and odd phase shift appears in the BM-TM amplitude and phase curves. The amplitude notches and odd phase variations of Fig. 4, 5, and 6, as well as the smaller phase variations observed Fig. 2, are reasonably attributable to such a scheme.

CONCLUSIONS

This study used two-tone stimulation and a dual pressure-voltage sensor to study cochlear amplification. Two stimulus paradigms were used, one a high-SPL, low-frequency suppressor with a swept-frequency probe tone and the other a paradigm in which the two tones were swept together at a fixed frequency ratio.

The results from the low-frequency suppressor paradigm supported our hypothesis regarding the amplifier-activating STV-STP phase shift: the phase shift was present even in fully suppressed conditions and therefore appears to be

based on passive mechanics, and somewhat adjustable by cochlear activity. In the results of the low-frequency suppressor paradigm, we observed a suppressor-induced shift in the amplitude of the STV responses at frequencies for which the mechanics (STP) was passive and unaffected by suppression. Those results reaffirm the mechano-transduction current as the locus of cochlear nonlinearity.

In the two-tone swept-frequency results, when the higher frequency tone (f_2) was in the vicinity of the measurement location's own BF, STV responses at f_1 were greatly attenuated, forming suppression notches. The analysis of the swept-frequency paradigm results supported the validity of fairly tightly coupled two-wave models of cochlear mechanics, which can easily generate the amplitude notches and phase variations that were apparent in our STV data. The schematic model used here (Fig. 8) generates predictions for differential motion that can be probed, for example, with OCT-based motion measurements within the organ of Corti. The OCT measurements to date have uncovered a variety of fairly tightly coupled motions and the relationship of those motions to OHC mechano-transduction current will guide our further understanding of hair cell excitation.

AUTHOR CONTRIBUTIONS

W.D. and E.S.O. contributed equally to the designing and execution of experiments and article preparation.

ACKNOWLEDGMENTS

We thank Mailing Wu and Polina Varavva for assistance with sensor development and construction.

This study was supported by National Institute on Deafness and Other Communication Disorders grants No. R01DC003130 and No. R01DC015362 (to E.S.O.) and R01DC011506 (to W.D.), and by the Emil Capita Foundation.

REFERENCES

1. Covell, W. P., and L. J. Black. 1936. The cochlear response as an index to hearing. *Am. J. Physiol.* 116:524–530.
2. Galambos, R., and H. Davis. 1944. Inhibition of activity in single auditory nerve fibers by acoustic stimulation. *J. Neurophysiol.* 7:287–303.
3. Cooper, N. P. 1996. Two-tone suppression in cochlear mechanics. *J. Acoust. Soc. Am.* 99:3087–3098.
4. Rhode, W. S., and N. P. Cooper. 1993. Two-tone suppression and distortion production on the basilar membrane in the hook region of cat and guinea pig cochleae. *Hear. Res.* 66:31–45.
5. Ruggero, M. A., L. Robles, and N. C. Rich. 1992. Two-tone suppression in the basilar membrane of the cochlea: mechanical basis of auditory-nerve rate suppression. *J. Neurophysiol.* 68:1087–1099.
6. Patuzzi, R., P. M. Sellick, and B. M. Johnstone. 1984. The modulation of the sensitivity of the mammalian cochlea by low frequency tones. III. Basilar membrane motion. *Hear. Res.* 13:19–27.
7. Geisler, C. D., and A. L. Nuttall. 1997. Two-tone suppression of basilar membrane vibrations in the base of the guinea pig cochlea using "low-side" suppressors. *J. Acoust. Soc. Am.* 102:430–440.
8. Geisler, C. D., G. K. Yates, …, B. M. Johnstone. 1990. Saturation of outer hair cell receptor currents causes two-tone suppression. *Hear. Res.* 44:241–256.
9. Rhode, W. S. 2007. Mutual suppression in the 6 kHz region of sensitive chinchilla cochleae. *J. Acoust. Soc. Am.* 121:2805–2818.
10. Versteegh, C. P., and M. van der Heijden. 2013. The spatial buildup of compression and suppression in the mammalian cochlea. *J. Assoc. Res. Otolaryngol.* 14:523–545.
11. Dong, W., and E. S. Olson. 2013. Detection of cochlear amplification and its activation. *Biophys. J.* 105:1067–1078.
12. Chen, F., D. Zha, …, A. L. Nuttall. 2011. A differentially amplified motion in the ear for near-threshold sound detection. *Nat. Neurosci.* 14:770–774.
13. Lee, H. Y., P. D. Raphael, …, J. S. Oghalai. 2015. Noninvasive in vivo imaging reveals differences between tectorial membrane and basilar membrane traveling waves in the mouse cochlea. *Proc. Natl. Acad. Sci. USA.* 112:3128–3133.
14. Lee, H. Y., P. D. Raphael, …, J. S. Oghalai. 2016. Two-dimensional cochlear micromechanics measured in vivo demonstrate radial tuning within the mouse organ of Corti. *J. Neurosci.* 36:8160–8173.
15. Cormack, J., Y. Liu, …, S. M. Gracewski. 2015. Two-compartment passive frequency domain cochlea model allowing independent fluid coupling to the tectorial and basilar membranes. *J. Acoust. Soc. Am.* 137:1117–1125.
16. Lamb, J. S., and R. S. Chadwick. 2014. Phase of shear vibrations within cochlear partition leads to activation of the cochlear amplifier. *PLoS One.* 9:e85969.
17. Lamb, J. S., and R. S. Chadwick. 2011. Dual traveling waves in an inner ear model with two degrees of freedom. *Phys. Rev. Lett.* 107:088101.
18. Kale, S., and E. S. Olson. 2015. Intracochlear scala media pressure measurement: implications for models of cochlear mechanics. *Biophys. J.* 109:2678–2688.
19. Olson, E. S. 1998. Observing middle and inner ear mechanics with novel intracochlear pressure sensors. *J. Acoust. Soc. Am.* 103:3445–3463.
20. Olson, E. S., and H. H. Nakajima. 2015. A family of fiber-optic based pressure sensors for intracochlear measurements. *Proc. SPIE.* 9303:163.
21. Dong, W., and E. S. Olson. 2008. Supporting evidence for reverse cochlear traveling waves. *J. Acoust. Soc. Am.* 123:222–240.
22. Olson, E. S. 2001. Intracochlear pressure measurements related to cochlear tuning. *J. Acoust. Soc. Am.* 110:349–367.
23. Fridberger, A., J. B. de Monvel, …, A. Nuttall. 2004. Organ of Corti potentials and the motion of the basilar membrane. *J. Neurosci.* 24:10057–10063.
24. Huang, S., and E. S. Olson. 2011. Auditory nerve excitation via a non-traveling wave mode of basilar membrane motion. *J. Assoc. Res. Otolaryngol.* 12:559–575.
25. Peterson, L. C., and B. P. Bogert. 1950. A dynamical theory of the cochlea. *J. Acoust. Soc. Am.* 22:369–381.
26. Olson, E. S. 2013. Fast waves, slow waves and cochlear excitation. *J. Acoust. Soc. Am.* 133:3508.
27. Dong, W., and E. S. Olson. 2009. In vivo impedance of the gerbil cochlear partition at auditory frequencies. *Biophys. J.* 97:1233–1243.
28. Johnson, S. L., M. Beurg, …, R. Fettiplace. 2011. Prestin-driven cochlear amplification is not limited by the outer hair cell membrane time constant. *Neuron.* 70:1143–1154.
29. Frank, G., W. Hemmert, and A. W. Gummer. 1999. Limiting dynamics of high-frequency electromechanical transduction of outer hair cells. *Proc. Natl. Acad. Sci. USA.* 96:4420–4425.
30. Engebretson, A. M., and D. H. Eldredge. 1968. Model for the nonlinear characteristics of cochlear potentials. *J. Acoust. Soc. Am.* 44:548–554.

31. Patuzzi, R. B., D. J. Brown, …, A. F. Halliday. 2004. Determinants of the spectrum of the neural electrical activity at the round window: transmitter release and neural depolarisation. *Hear. Res.* 190:87–108.

32. Fahey, P. F., B. B. Stagner, …, G. K. Martin. 2000. Nonlinear interactions that could explain distortion product interference response areas. *J. Acoust. Soc. Am.* 108:1786–1802.

33. Cheatham, M. A., and P. Dallos. 1982. Two-tone interactions in the cochlear microphonic. *Hear. Res.* 8:29–48.

34. Cheatham, M. A., and P. Dallos. 1992. Two-tone suppression in inner hair cell responses: correlates of rate suppression in the auditory nerve. *Hear. Res.* 60:1–12.

35. Cheatham, M. A., and P. Dallos. 1992. Physiological correlates of off-frequency listening. *Hear. Res.* 59:39–45.

36. Zweig, G. 1991. Finding the impedance of the organ of Corti. *J. Acoust. Soc. Am.* 89:1229–1254.